Bipolar TiO_2/Pt Semiconductor Photoelectrodes and Multielectrode Arrays for Unassisted Photolytic Water Splitting

Eugene Smotkin, Allen J. Bard,* Alan Campion, Marye A. Fox, Thomas Mallouk, Stephen E. Webber, and J. M. White

Department of Chemistry, The University of Texas, Austin, Texas 78712 *(Received: January 30, 1986)*

Bipolar TiO_2/Pt photoelectrodes were fabricated by anodization of thin Ti foils onto which Pt had been previously sputter-deposited. These photoelectrodes are capable of a vectorial charge transfer. Current-potential curves were used to predict the behavior of multielectrode arrays. Several different multielectrode cells, utilizing KOH, O_2 electrolytes, were constructed. In series configuration, the open-circuit voltage V_{oc} is proportional to the number of panels used. With five panels in series, a V_{oc} in excess of 3.6 V is obtained, permitting unassisted photolytic (Xe lamp) water splitting to produce H_2 and O_2.

Introduction

Connecting several photoactive junctions in series[1] will generate a sufficient driving force to decompose H_2O to H_2 and O_2 without an external bias. We describe here the construction of bipolar electrodes consisting of a polycrystalline film of TiO_2 formed by spark anodization of Ti with a sputtered Pt backing (denoted TiO_2//Pt) and the series assembly of these into multipanel arrays that split water when irradiated with a xenon lamp.

Studies of water photoelectrolysis ("water splitting") with TiO_2 and Pt electrodes date from the work of Honda and Fujishima.[2] Because the potential developed by this pair is inadequate to drive the water-splitting reaction at a useful rate, an external bias must be applied. This bias can be either an external electrical potential or a chemical bias established by contacting the TiO_2 with a strong alkaline and the Pt with a strong acidic solution.[3] In such cases an expenditure of energy in addition to the incident radiant (e.g., solar) energy is required. An alternative strategy involves the utilization of one or more PEC cells to bias the water-splitting cell. Earlier work[1] showed, for example, that this could be accomplished by coupling of Texas Instruments solar energy system arrays based on Si p/n junctions. Simpler types of bipolar electrodes, and arrays based on these, have not previously been described.

The bipolar electrodes described here utilized polycrystalline TiO_2 films. Thin-film photoelectrodes, (e.g., produced by chemical vapor deposition,[4] thermal oxidation,[5,6] anodic oxidation,[7,8] RF sputtering,[9] and sol-gel methods[10]) have been reported. We adopted the anodic film approach here, because such films can be readily and reproducibly produced on thin Ti foils faced with sputtered Pt films. Such bipolar TiO_2//Pt electrodes (where // represents an ohmic contact) are capable of vectorial charge transfer, with photogenerated holes (h^+) moving to the TiO_2 interface to cause an oxidation and the electrons (e^-) moving to the Pt interface to carry out a reduction. The energetics of such a bipolar electrode follow directly from the well-established principles of PEC cells[11] as shown schematically in Figure 1. The analysis of the electrochemical behavior of a single bipolar electrode for actual redox couples and of series connected multijunction cells can be carried out by graphical addition of current-potential (i-V) curves,[1] as described below.

Experimental Section

Photosensitive TiO_2 films were prepared by the high-voltage anodization technique reported by Marchenoir et al.[12] and Miller.[7] The Ti foil, purchased from Johnson Matthey, Inc., had a thickness of 0.025 mm and a purity of 99.7%. The Ti foil was degreased in methylene chloride and rinsed in distilled water. One side of the foil was coated with a Pt film ca. 350 nm thick by RF sputtering with a Materials Research Co. (Orangeburg, NY) Model 8620 sputtering apparatus at 2×10^{-2} Torr of Ar with a deposition rate of 10 Å/s. The platinized foil was cut into 3- × 3-cm squares, and the Ti side was subjected to spark anodization in the cell shown in Figure 2. Sulfuric acid (2.5 M) was used as the electrolyte facing the Ti side with a platinized titanium foil serving as the cathode. Side B, facing the Pt, was filled with ice water to cool the electrode during the anodization. The Ti foil, which served as the anode, was glued between the cells with silicone cement. The voltage between the Ti foils was gradually increased with the current density never exceeding 35 mA/cm^2. Sparking began at 95 V and continued up to the final applied voltage, 125 V; at this point the electrolyte was replaced and the final voltage maintained for 10 min. The anodized foil, with a TiO_2 film thickness of 2 μm, was rinsed in boiling distilled water before use. The thickness of TiO_2 films formed on anodization depended upon the applied voltage;[13] thicknesses of anodized films were estimated from scanning electron micrographs.

Voltammograms were recorded with a Princeton Applied Research (PAR) Model 173 potentiostat/galvanostat, a PAR Model 175 universal programmer, and a Houston Instruments Model 2000 X-Y recorder. The illumination source was a 2500-W xenon lamp from which infrared wavelengths were removed by an 8-in. water filter. The photon flux, measured with a Coherent light meter, was 266 mW/cm^2. Open-circuit voltages were measured with a Fluke Model 8060 A multimeter. All chemicals were reagent grade and were used without further purification.

Power characteristics of the PEC cells were evaluated by employing the potentiostat as a variable load; the counter and reference electrode leads of the PAR were connected to a platinum electrode, and the illuminated TiO_2 electrode was connected to the working electrode lead. The applied potential was then decreased from 0 V (to yield the short-circuit current, i_{sc}) until the current ceased (to yield the open-circuit photovoltage, V_{oc}).

The cell for multipanel series configurations was constructed from a Pyrex tube (15 mm) cut at 4-cm intervals at 45° angles. Each segment had a filling port through which electrolyte could be added. The electrodes were glued between the segments with

(1) White, J. R.; Fan, F.-R. F.; Bard, A. J. *J. Electrochem. Soc.* **1985**, *132*, 544.
(2) Fujishima, A.; Honda, K. *Nature (London)* **1972**, *238*, 37.
(3) Wrighton, M. S. *Proc. Natl. Acad. Sci. U.S.A.* **1975**, *72*, 1518.
(4) (a) Hardee, K. L.; Bard, A. J. *J. Electrochem. Soc.* **1975**, *122*, 739. (b) Laser, D.; Bard, A. J. *J. Electrochem. Soc.* **1976**, *123*, 1027. (c) Takahashi, Y. *J. Chem. Soc., Faraday Trans. 1* **1981**, *77*, 1051.
(5) Hartig, K. J.; Getoff, N. *Int. J. Hydrogen Energy* **1983**, *8*, 603.
(6) Matsumoto, Y. *Electrochim. Acta* **1982**, *27*, 419.
(7) Miller, D. *Chem. Phys. Lett.* **1983**, *100*, 236.
(8) Getoff, N. *Sol. Energy Mater.* **1983**, *9*, 167.
(9) Lakshmanan, T. K.; Wysocki, C. A. *IEEE Trans. Compon. Parts* **1964**, *CP-11*, 14.
(10) Yoko, T.; Kamiya, K. Tanimoto, K.; Kimura, S.; Sakka, S. Proceedings of the 5th International Conference on Photochemical Conversion and Storage of Solar Energy, Osaka, Japan, 1984; Abstract B15(6).
(11) Bard, A. J. *Science* **1980**, *207*, 139.
(12) Marchenoir, C. *Thin Solid Films* **1980**, *66*, 357.
(13) Mizushima, W. *J. Electrochem. Soc.* **1961**, *108*, 825.

0022-3654/86/2090-4604$01.50/0

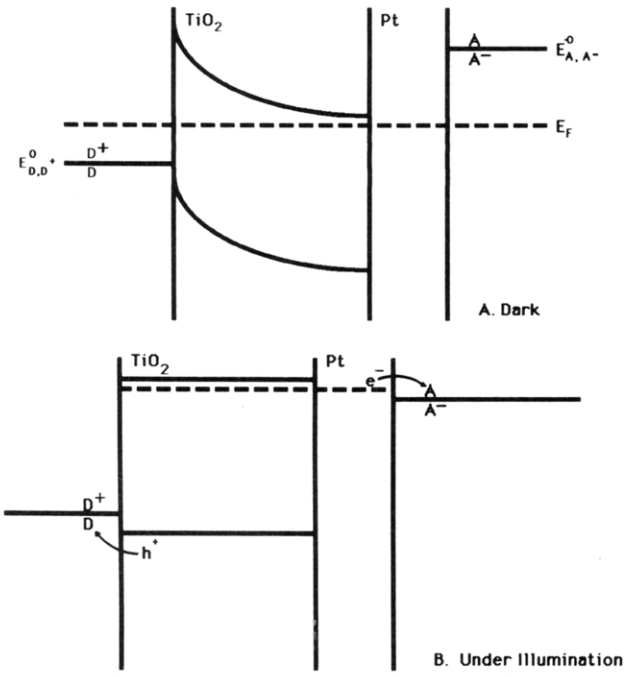

Figure 1. Schematic representation of TiO_2//Pt bipolar electrode in contact with solutions containing the D^+,D and A,A^- couples (A) in the dark at equilibrium and (B) under irradiation.

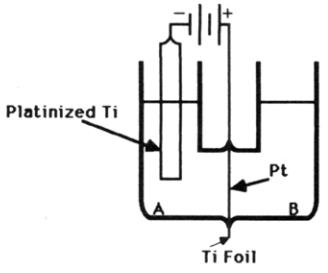

Figure 2. Anodization cell. Side A contains anodizing electrolyte (2.5 M H_2SO_4) in contact with Ti surface to be anodized, with a platinized Ti counter electrode. Side B contains ice water in contact with platinized Ti surface.

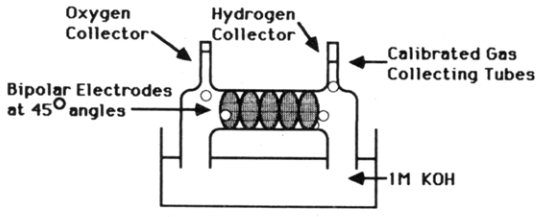

Figure 3. Water photoelectrolysis cell with five bipolar electrodes in series showing semiconductor faces of electrodes.

epoxy (Ring Chemical Co., Houston, TX) with all of the platinum sides facing in the same direction. The five-panel water photoelectrolysis system is shown in Figure 3 with the TiO_2 faces showing. The end cells were filled by complete immersion of the cell into a 1 M KOH bath. The interior cells were then filled to desired levels through the ports. An oxygen atmosphere was maintained above the electrolyte in the interior cells. The gas-collecting tubes on the end cells were calibrated to permit monitoring of gas volume with time. The evolution of hydrogen and oxygen was confirmed by gas chromatographic analysis using a column packed with 50 g of 13 X, 60/80-mesh sieves from Alltech Associates Inc., with argon as the carrier gas at 30 mL/min.

Results and Discussion

Photoelectrochemical Behavior of Single TiO_2//Pt Panels. The TiO_2 films formed by anodization were about 2 μm thick with pore diameters of about 1000 Å (Figure 4). X-ray diffraction measurements showed powder patterns characteristic of both rutile and anatase phases as well as Ti_2O_3, TiO, and Ti metal, suggesting a gradient of oxides with the lower oxides nearer the Ti surface. One form of bipolar electrode consisted of a free-standing TiO_2 film produced by spark anodizing the Ti foil to form a TiO_2 film, RF sputtering of Pt onto the TiO_2, and dissolving the remaining Ti substrate in methanol containing 20% Br_2. The resulting TiO_2/Pt film was handled with Nylon mesh. However, it was easier to platinize the Ti before anodization of the opposite side, and this configuration was used in all of the experiments described below.

The photoelectrochemical behavior of the bipolar panel was elucidated by studying the i–V characteristics of each side independently. For this purpose the panel was clamped between two solutions in the configuration of Figure 2. The resulting i–V curves for the interfaces TiO_2/KOH (A1), Pt/KOH, O_2 (O1), and Pt/KOH (H1, deaerated with Ar) are shown in Figure 5 (where an asterisk indicates an irradiated surface). These are the familiar curves for photogeneration of O_2 on TiO_2, the reduction of O_2 on Pt, and the reduction of H_2O on Pt to produce H_2, respectively.[2-4] The current–time behavior at the Pt/KOH, O_2 interface strongly depended upon the way the interface was established, as seen previously in PEC cells.[14] When the entire Pt electrode was immersed in the O_2-saturated solution, the current quickly decayed with time as the low initial concentration of O_2 near the electrode was depleted (Figure 6, curve A). Higher currents could be sustained by partial immersion of the Pt side and allowing gaseous O_2 to diffuse through the thin electrolyte solution meniscus; this resulted in more effective transport of O_2 to the electrode (curve B). This configuration was used in the PEC cells, since in this form currents were limited by the incident radiation intensity rather than by the O_2 mass-transfer rate in solution. These results demonstrate the importance in designing both interfaces of the bipolar electrode to maximize the photocurrent.

Multielectrode O_2/OH^- Cells. To demonstrate vectorial charge transfer at a panel, the cell compartments on either side of the bipolar film shown in Figure 2 were equipped with two large Pt foil electrodes and were each filled with O_2-saturated KOH, i.e.

$$+\ Pt/KOH,O_2/*TiO_2//Pt/KOH,O_2/Pt\ -$$

Upon irradiation of the TiO_2 side of the bipolar electrode, an open-circuit photovoltage of 0.81 V and a short-circuit current of 0.4 mA were produced between the immersed Pt foils. This open-circuit voltage falls within the range of reported values.[2,14] A quantitative investigation of open-circuit photovoltages and causes for variabilities has been reported.[15] This short-circuit current does not represent the maximum current attainable at a single bipolar electrode, since Pt electrodes (found at each end of this assembly) show overpotentials for the O_2 evolution and O_2 reduction reactions (in addition to iR drop through the solution). The maximum bipolar electrode current can be estimated by consideration of the A1 and O1 i–V curves in Figure 6. The short-circuit photocurrent, i_{sc}, occurs where the cathodic and photoanodic currents are equal (as indicated in Figure 6 at the mixed potential, E_{M1}). The open-circuit photovoltage (V_{oc} = 0.82 V) is obtained as the potential difference when both currents are zero.

The predicted i–V curves for panels in series (Figure 3) are given in Figure 7. These can be obtained by independent graphical addition of the cathodic curves by summing the potentials at constant current (since the electrodes are connected in series), and treating in the same way, the anodic ones. The result of this procedure, in consideration of a two-panel cell with both Pt cathodes immersed in O_2-saturated KOH, is shown in Figure 7 as curves A2 and O2. The power curves for the multiple panels in series were obtained by using the cell in Figure 3. Three panels were used with two intervening electrolyte solutions:

$$Pt//TiO_2*//KOH,O_2/Pt//TiO_2*/KOH,O_2/Pt$$

(14) Keeney, J.; Weinstein, D. H.; Haas, G. M. *Nature (London)* **1975**, *253*, 719.
(15) Lewis, N. *J. Electrochem. Soc.* **1984**, *131*, 2496.

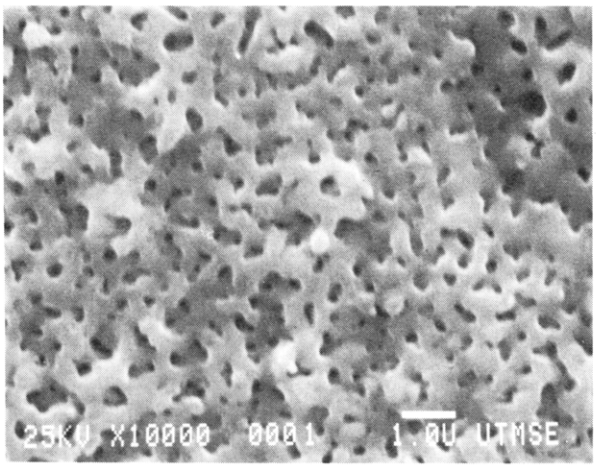

Anodized TiO_2 surface

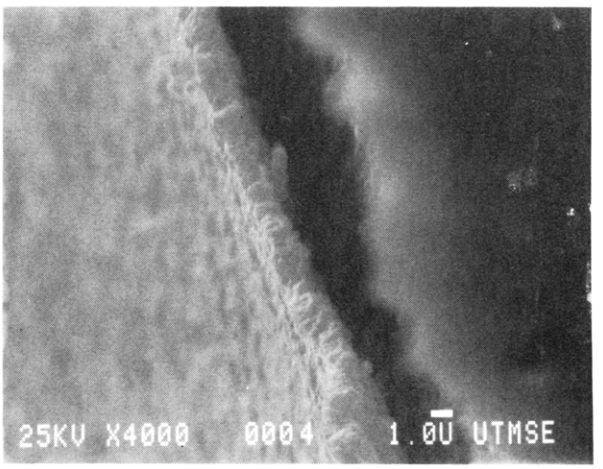

TiO_2/Ti interface

Figure 4. Scanning electron micrographs of anodized TiO_2 surface and TiO_2/Ti interface.

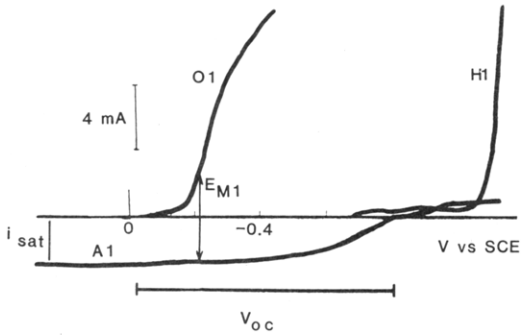

Figure 5. Current–potential curves for irradiated TiO_2/KOH (A1), Pt/KOH, O_2 (O1), and Pt/KOH (deaerated) (H1).

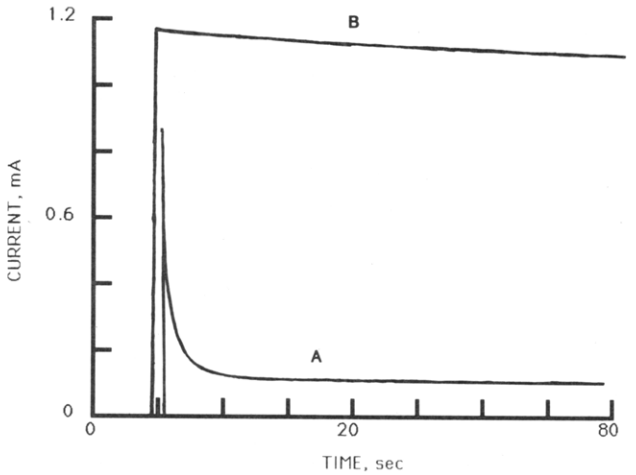

Figure 6. Current vs. time profiles for illuminated TiO_2 surface (5.7 cm^2) with Pt counter electrode in 1 M KOH: curve A, counter electrode completely immersed; curve B, counter electrode partially immersed.

The experimental results are shown in Figure 8. The behavior of cells with four and five panels can be deduced in a similar way from the i–V curves; those for three active panels are shown as curves O3 and A3 in Figure 7. The experimental results for one- through four-panel PEC cells are shown in Table I. As expected, the V_{oc} of the cells are additive and the i_{sc} values are constant (within the small variability among the panels). Thus, the efficiency of the overall cell is independent of the number of panels (Table I).

Water Photoelectrolysis Cell. The individual i–V curves for TiO_2/KOH (A1) and Pt/KOH (deaerated) (H1) when combined

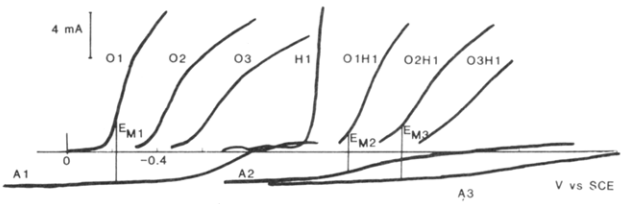

Figure 7. Current–potential characteristics of TiO_2//Pt panels in 1 M KOH: O1, oxygen reduction wave, Pt/KOH, O_2; O2, sum of two O1 curves yielding reduction wave for two panels; O3, sum of three O1 curves yielding reduction wave for three panels; H1, reduction wave for single panel in outgassed KOH solution; O1H1, reduction wave for H1 biased by O1; O2H1, reduction wave for H1 biased by two O1 panels; A1, anodic photocurrent for single panel; A2, anodic photocurrent for two panels in series; A3, anodic photocurrent for three panels in series.

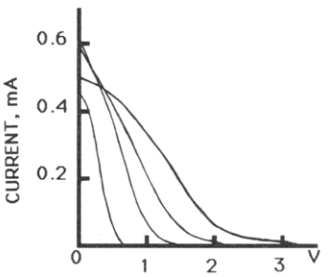

Figure 8. Power curves for TiO_2/Pt panels in series (panel area 1.0 cm^2, in 1 M KOH with oxygen atmosphere, 266 mW/cm^2 xenon lamp illumination).

TABLE I: Power Characteristics

	no. of panels			
	1	2	3	4
fill factor (ff)	0.46	0.41	0.38	0.44
V_{oc}, V	0.73	1.5	2.3	3.1
i_{sc}, mA	0.45	0.6	0.56	0.5
overall efficiency,[a] %	0.057	0.069	0.061	0.064

[a] Calculated by $ff V_{oc} i_{sc}/PAn$, where P is flux, A is area of panel, and n is the number of panels. Photon flux (xenon lamp) 266 mW/cm^2, exposed area 1 cm^2.

clearly show that a single panel cannot drive the water-splitting reaction. However, by utilizing interior panels in O_2-saturated solution to provide a bias, one can attain a sufficient driving force for H_2 and O_2 production. Consider the two-panel cell

KOH[1] ×
(deaerated)/Pt//TiO_2*/KOH[2]O_2/Pt//TiO_2*,KOH[3]

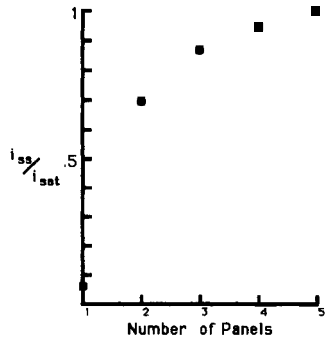

Figure 9. i_{sc}/i_{sat} vs. number of panels (1 cm^2) in 1 M KOH.

where the two ends of the cell (KOH solutions [1] and [3]) are connected by a KOH salt bridge. The predicted behavior of this cell can be derived from addition of two A1 curves to yield A2 and the addition of O1 to H1 to yield O1H1 (Figure 7). The rate of H_2 and O_2 evolution can be estimated from the power curve derived by addition of these. The characteristics of a three-panel cell can similarly be derived by consideration of curves A3 and O2H1. Note that the predicted i_{sc} for the two-panel cell is less than the radiation-limited current (i_{sat}), but for the three-panel cell $i_{sc} = 0.85i_{sat}$. A plot of i_{sc}/i_{sat} vs. number of panels, shown in Figure 9, suggests that, for conversion of solar energy to H_2 and O_2, there is little to be gained in using a configuration with more than three panels. However, to test the operation of a multiple-panel PEC cell for water splitting, a five-panel cell, shown in Figure 3, was illuminated for 5 h with a Xe lamp (266 mW/cm^2 incident). Gas evolution occurred at each end electrode, H_2 being evolved on the Pt extreme and O_2 at the TiO_2 end. A volume of 0.52 mL of H_2 (identified by gas chromatography) evolved, and an H_2/O_2 molar ratio of 2.4/1 was obtained. The deficiency in the amount of O_2 generated as compared to that expected from the decomposition of H_2O on TiO_2 has been attributed to the formation of peroxides.[16,17]

Conclusions

Vectorial charge transfer on bielectrode panels has been demonstrated. Means have been established for coupling these panels to produce higher driving forces than those available from systems with single semiconductor electrodes and for predicting the PEC characteristics from individual i–V curves. The unassisted photolytic water-splitting reaction has been demonstrated. No effort was made in these studies to optimize the behavior of the PEC cells through improvement of the TiO_2 film, new interior redox couples, or better mass transport. Such improvements and alternative semiconductor materials are currently under investigation in these laboratories.

Acknowledgment. The support of this research by the Gas Research Institute is gratefully acknowledged.

Registry No. TiO_2, 13463-67-7; KOH, 1310-58-3; Ti_2O_3, 1344-54-3; TiO, 12137-20-1; H_2O, 7732-18-5; H_2, 1333-74-0; O_2, 7782-44-7; Pt, 7440-06-4; Ti, 7440-32-6.

(16) Duonghong, D.; Gratzel, M. *J. Chem. Soc., Chem. Commun.* **1984**, *23*, 1597.
(17) Muraki, H.; Saji, T.; Fujihara, M.; Aoyagui, S. *J. Electroanal. Chem.* **1984**, *169*, 319.

A TPD/AES Study of the Interaction of Dimethyl Methylphosphonate with α-Fe_2O_3 and SiO_2

M. A. Henderson, T. Jin, and J. M. White*

Department of Chemistry, University of Texas, Austin, Texas 78712 *(Received: February 14, 1986)*

The interaction of dimethyl methylphosphonate (DMMP) dosed at 170 K onto SiO_2 and α-Fe_2O_3 was studied by temperature programmed desorption (TPD) and Auger electron spectroscopy (AES). On dehydrated SiO_2 there was no DMMP decomposition and there were two DMMP TPD peaks, a multilayer state at 200–210 K and a monolayer state at 275 K. On hydrated SiO_2 no more 10% of a monolayer of DMMP decomposed and the only detectable TPD products were methylphosphonate (MP) and methanol. On clean α-Fe_2O_3 multilayer DMMP was observed but no molecular peak corresponding to the monolayer. Decomposition led to CO_2, CO, CH_3OH, HCOOH, H_2, H_2O, and an adsorbed phosphate species. The presence of the phosphate species did not completely inhibit the decomposition of subsequent doses of DMMP even after saturation of the AES P(114)/Fe(703) signal ratio at 0.45 to 0.55. The AES P(114)/Fe(703) signal ratio decreased at temperatures above 600 K. Migration of the phosphorus to an iron oxide–phosphate phase below the surface is proposed to explain the continued DMMP decomposition.

Introduction

The purpose of this paper is to report recent findings in this laboratory for the interaction of dimethyl methylphosphonate (DMMP) with the surfaces of SiO_2 and α-Fe_2O_3. In previous work involving the adsorption of DMMP on clean and carbon-covered Rh(100),[1] the bonding of DMMP to the Rh surface was assigned to interactions through the lone pair of electrons on the oxygen of –P=O. Only a small fraction of the molecularly adsorbed DMMP desorbed from an initially clean Rh(100) surface during TPD experiments. The remainder decomposed to small molecules including H_2, H_2O, CO, CO_2, CH_4, and CH_3OH. In addition to these decomposition products, AES at 500 K detected the presence of P, C, and O on the surface following DMMP decomposition. In contrast to the clean Rh(100) surface, no DMMP decomposition was observed on a carbon-covered Rh(100) surface.

In related work, Weinberg and Templeton have recently studied the interaction of DMMP with Al_2O_3 using inelastic electron tunneling spectroscopy (IETS).[2] They observed the stepwise decomposition of chemisorbed DMMP dosed at 200 K to methyl methylphosphonate (MMP) above 295 K and to methylphosphonate (MP) above 573 K, each step resulting in the loss of a methoxyl group.

In this work, we have studied the interaction of DMMP with the surfaces of SiO_2 and α-Fe_2O_3 using temperature programmed desorption (TPD) and Auger electron spectroscopy (AES).

(1) Hegde, R. I.; Greenlief, C. M.; White, J. M. *J. Phys. Chem.* **1985**, *89*, 2886.

(2) (a) Templeton, M. K.; Weinberg, W. H. *J. Am. Chem. Soc.* **1985**, *107*, 97. (b) Ibid. **1985**, *107*, 774.

0022-3654/86/2090-4607$01.50/0